

Comparison of Linear Time-Invariant and Linear Time-Periodic Models for Small-Signal Stability Analysis of Power Electronic Converters

Özgür Can Sakinci*, Jef Beerten

KU Leuven, Dept. ESAT, ELECTA Research Group & EnergyVille, 3001 Leuven Belgium

Email: *ozgurcan.sakinci@kuleuven.be

Abstract—This paper presents a comparison of two different frameworks to develop linear averaged state-space models of power electronic converters: linear time-invariant framework and linear time-periodic framework. Small-signal stability analysis methods that accompany the aforementioned frameworks are introduced and compared in terms of their applicability to power-electronics based systems. Both frameworks are applied to a two-level voltage-source converter, and the results of a stability study are introduced. It is shown how models developed using both frameworks can effectively capture the small-signal behavior of the converter if certain parameters are varied.

Index Terms—linear time-invariant, linear time-periodic, small-signal stability, power electronics, state-space model

I. INTRODUCTION

With the global incentives towards more renewable energy generation pushing the installment of wind turbines and PV installations and the advances in the power electronic industry enabling high-power semiconductor-based grid control elements, the amount of power electronics connected to the electricity grid is showing a rapid increase over the past years. Also for power transmission, high-voltage direct-current (HVDC) transmission systems based on voltage-source converters (VSC) composed of several hundreds of semiconductor switches are becoming increasingly popular, since they allow flexible power transmission and control. From the system operators' point of view, the increasing usage of power electronic devices provides numerous advantages, but at the same time makes the analysis of the system stability more challenging. One of the main challenges is related to ensuring the small-signal stability of the system. High switching frequencies of the VSCs result in interactions with the power system at higher frequencies, which are ignored during traditional power system small-signal stability assessment. To tackle such undesired interactions, many small-signal stability analysis methods exist in the literature. Within these methods, the impedance-based stability criterion and eigenvalue analysis are commonly applied [1]. Although the impedance-based stability criterion can evaluate the stability of two connected systems at the connection interface by applying the Nyquist stability criterion, it is a local method and lacks further analysis techniques since the instabilities cannot easily be traced to certain state variables.

Traditional power system small-signal stability analysis mainly relies on the calculation of the eigenvalues of the system matrix, which gives insight on the global stability of the system, and the effect of different state variables on stability [2]. To overcome discontinuities at system states due to the switching action of the converters, averaged models are used, which generally result in linear time-invariant (LTI) systems, enabling the usage of system eigenvalues to assess the stability. Because of the periodic nature of most power system states, some converter topologies cannot be easily represented as an LTI system. In that case, it is usually more beneficial to model the system as a linear time-periodic (LTP) one, and to

carry out the stability analysis of such systems [3]. Depending on the chosen modeling framework, both LTI and LTP models of the same converter can be developed. However, stability analysis of power electronic converters using LTP models has not been extensively implemented, mainly due to the post-processing methods being not as straightforward as the LTI case.

In light of the challenges described above, this paper carries out a comparative study of small-signal stability analysis of linearized state-space models obtained using the LTI and LTP frameworks. Section II presents a general introduction to the theory of small-signal stability analysis using both frameworks, general assumptions that accompany the development of such models and their limitations. In Section III, time-invariant and time-periodic models of a two-level VSC and its current controllers are developed. Section IV presents the linearization of both models, and a stability study in which the controller gains are varied to observe their effect on the small-signal stability of the VSC. Section V discusses the effect of the chosen controller architecture on the modeling framework to be used and finally, Section VI draws the conclusions of the paper, and provides further points towards future research on the application of the LTP framework.

II. SMALL-SIGNAL STABILITY ASSESSMENT

The small-signal stability of a system can be defined as the ability of the system to return to a stable equilibrium point when it is subjected to a small disturbance. For linear systems, if the state vector and the input vector are written as a linear superposition of their small-signal components $\Delta\vec{x}(t)$ & $\Delta\vec{u}(t)$ and steady-state components $\vec{x}_0(t)$ & $\vec{u}_0(t)$ as:

$$\vec{x}(t) = \Delta\vec{x}(t) + \vec{x}_0(t) \quad \& \quad \vec{u}(t) = \Delta\vec{u}(t) + \vec{u}_0(t) \quad (1)$$

then the small-signal dynamics of the system are governed by the following state-space equation:

$$\Delta\dot{\vec{x}}(t) = \mathbf{A}(t)\Delta\vec{x}(t) + \mathbf{B}(t)\Delta\vec{u}(t) \quad (2)$$

where the matrices $\mathbf{A}(t)$ and $\mathbf{B}(t)$ define the system dynamics for the system state vector $\vec{x}(t)$ and the input vector $\vec{u}(t)$. For LTI systems, which satisfy $\frac{d}{dt}\mathbf{A}(t) = 0$, the system is stable in the small-signal sense if $\mathbf{A}(t)$ has all its eigenvalues in the left-half plane.

For most of the three-phase power system equipments (including VSCs), the first step during modeling to obtain an LTI system is to apply averaging based on the switching period. This is common practice in system-level studies, since instead of the high-frequency switching phenomena, the slow transients are the main concern. By replacing the switched signals with their moving average as [4]:

$$\bar{x}(t) = \frac{1}{T_s} \int_{t-T_s}^t x(\tau) d\tau \quad (3)$$

where T_s is the constant switching period, one can focus on the slow-varying dynamics, instead of the high-frequency switching behavior. Doing so, average models allow to replace the switching with a controlled source, making it easier to analyze the system [4].

When the switching effects are removed by applying averaging, the analysis of the eigenvalues of the system matrix is usually enough to arrive at a statement regarding the small-signal stability of the system. Moreover, by means of the left and right eigenvectors, eigenvalue analysis also provides information about states that can be used to control a certain oscillatory mode, and in which system states a certain mode can be observed, respectively [2].

If the system is time-varying, however, the eigenvalues of the system matrix $\mathbf{A}(t)$ cannot be used to judge the system stability. For LTP systems, a special class of time-varying systems that satisfy $\mathbf{A}(t+T) = \mathbf{A}(t)$ for a certain period T , the stability of the system can be analyzed by using the Floquet-Lyapunov theory. The theory makes use of the state transition matrix $\Phi(t_1, t_2)$ of the system, which defines the evolution of the system states from time t_1 to t_2 as:

$$\vec{x}(t_2) = \Phi(t_1, t_2)\vec{x}(t_1) \quad (4)$$

For the system to be stable in the small-signal sense, the monodromy matrix—the state transition matrix after one period—, $\Phi(T, 0)$, needs to have its eigenvalues inside the unit circle [3]. The eigenvalues of the monodromy matrix are also called *Poincaré multipliers* [3]. The stability analysis of LTP systems is relatively straightforward, yet it is generally perceived to be less powerful than the stability analysis of LTI systems, because of the lack of widespread post-processing tools such as eigenvectors and participation factors [2]. Moreover, an inherent challenge exists when the monodromy matrix is to be calculated during stability analysis. As the complexity of the system increases, it gets harder to arrive at a closed-form analytical expression for the monodromy matrix, or such an expression might even be non-existent [5]. Alternatively, the monodromy matrix can be numerically calculated by following the steps below:

Step 1: For a system with N states, the equation $\Delta\dot{\vec{x}}(t) = \mathbf{A}(t)\Delta\vec{x}(t)$ needs to be solved for N independent initial conditions. The N different initial conditions, $\vec{x}_1(0), \dots, \vec{x}_N(0)$, which produce the solutions $\vec{x}_1(T), \dots, \vec{x}_N(T)$ after one period of $\Phi(T, 0)$, are obtained as the independent columns of the $N \times N$ identity matrix. **Step 2:** Once the solutions are calculated through numerical integration, the monodromy matrix is obtained as:

$$\Phi(T, 0) = [\vec{x}_1(T)|\vec{x}_2(T)|\dots|\vec{x}_N(T)]$$

The LTP framework utilizing the Poincaré multipliers for small-signal stability assessment has previously been applied by many researchers to conduct stability studies of switched power-electronic converters. Mazumder *et al.* presented a comparison of an averaged model with a model that accurately models the switching behavior of a single-phase bidirectional boost converter, and discovered fast-scale instabilities by analyzing the Poincaré multipliers [6]. This instability was not captured by the averaged model due to the exclusion of the switching behavior. In a similar fashion, possible bifurcations leading to structural instabilities in a DC-DC resonant converter have been analyzed by means of its Poincaré multipliers in [7]. Such an analysis of the Poincaré multipliers was able to detect controller gains that result in an unstable converter.

III. CONVERTER MODEL

As an example, the concepts introduced in the previous section are illustrated on a standard three-phase two-level VSC. The LTI framework is applied after the application of Park transform which

results in variables in the rotating DQ frame, and the LTP framework is applied to the variables in the stationary ABC frame. The converter is modeled together with a simplified AC grid representation, an LCL filter and the DC-side capacitor. A current controller controls the converter current i_c with PI controllers in the DQ frame. It is assumed that a perfect PLL is present, which tracks the grid voltage angle to perform the Park transform. The converter topology, including the AC-side representation with the filter, is depicted in Fig. 1.

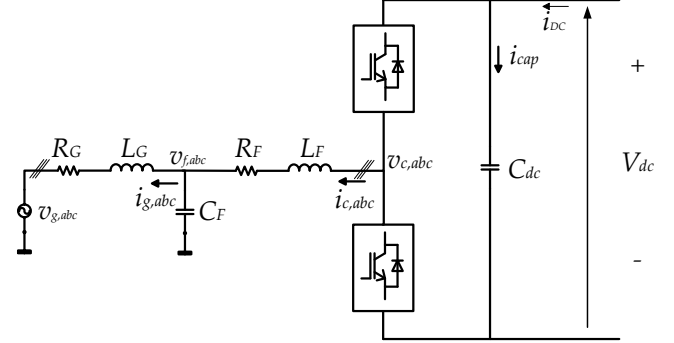


Fig. 1. Three-phase two-level VSC topology

A. Time-Periodic Modeling

An averaged model is being used, which implies that the terminal voltage of the converter for an arbitrary phase j , v_{cj} , is given as:

$$v_{cj} = m_j \frac{v_{dc}}{2} \quad (5)$$

where $m_j \in \{0, 1\}$ is the modulation index of phase j . The per-phase operation of the converter is then modeled by using four state variables: the AC-side current i_g , converter current i_c , LCL filter voltage v_f and DC voltage v_{dc} . The corresponding equations guiding the derivatives of these state variables for an arbitrary phase j are defined as follows:

$$L_G \frac{di_{gj}}{dt} = v_{fj} - v_{gj} - R_G i_{gj} \quad (6a)$$

$$L_F \frac{di_{cj}}{dt} = v_{cj} - v_{fj} - R_F i_{cj} \quad (6b)$$

$$C_F \frac{dv_{fj}}{dt} = i_{cj} - i_{gj} \quad (6c)$$

$$C_{dc} \frac{dv_{dc}}{dt} = i_{cap} \quad (6d)$$

In its current form, (6) does not completely model the two-level VSC, since the power balance between the AC & DC sides needs to be defined to arrive at an expression for the capacitor current. This power balance is defined as:

$$v_{dc}(i_{dc} - i_{cap}) = v_{ca}i_{ca} + v_{cb}i_{cb} + v_{cc}i_{cc} \quad (7a)$$

$$i_{cap} = \frac{v_{dc}i_{dc} - v_{ca}i_{ca} - v_{cb}i_{cb} - v_{cc}i_{cc}}{v_{dc}} \quad (7b)$$

The substitution of i_{cap} with (7b) and v_{cj} with (5) completes the per-phase state-space description of the two-level VSC. For a three-phase VSC, the model consists of ten state variables. It contains multiplications of system states, thus it is nonlinear. After linearization, since the modulation indices m_j are sinusoidal signals, \mathbf{A} becomes a periodic matrix. Therefore, the model naturally becomes a time-periodic one in the ABC frame if no precautions are taken to overcome the periodicity.

B. Time-Invariant Modeling

In steady state, the modulation indices are fundamental-frequency sinusoids calculated by the current controller. To arrive at a time-invariant model, the model can be developed in the rotating DQ frame, since the fundamental-frequency sinusoids become constants in the DQ frame. A power-variant Park transform is used, with the transformation matrix given by:

$$T_{Park} = \frac{2}{3} \begin{bmatrix} \cos(\omega t) & \cos(\omega t - 2\pi/3) & \cos(\omega t - 4\pi/3) \\ \sin(\omega t) & \sin(\omega t - 2\pi/3) & \sin(\omega t - 4\pi/3) \end{bmatrix} \quad (8)$$

In terms of the DQ variables, the converter terminal voltages are written as:

$$\vec{v}_{c,dq} = \vec{m}_{dq} \frac{v_{dc}}{2} \quad (9)$$

The power balance in terms of the DQ variables is written as:

$$v_{dc}(i_{dc} - i_{cap}) = \frac{3}{2} (v_{cd}i_{cd} + v_{cq}i_{cq}) \quad (10a)$$

$$i_{cap} = i_{dc} - \frac{3}{2} \left(\frac{m_d i_{cd}}{2} + \frac{m_q i_{cq}}{2} \right) \quad (10b)$$

By using (10b), the model in the DQ frame which has eight state variables is written as:

$$L_G \frac{d\vec{i}_{g,dq}}{dt} = \vec{v}_{f,dq} - \vec{v}_{g,dq} - R_G \vec{i}_{g,dq} - L_G \begin{bmatrix} 0 & \omega \\ -\omega & 0 \end{bmatrix} \vec{i}_{g,dq} \quad (11a)$$

$$L_F \frac{d\vec{i}_{c,dq}}{dt} = \vec{v}_{c,dq} - \vec{v}_{f,dq} - R_F \vec{i}_{c,dq} - L_F \begin{bmatrix} 0 & \omega \\ -\omega & 0 \end{bmatrix} \vec{i}_{c,dq} \quad (11b)$$

$$C_F \frac{d\vec{v}_{f,dq}}{dt} = \vec{i}_{c,dq} - \vec{i}_{g,dq} - C_F \begin{bmatrix} 0 & \omega \\ -\omega & 0 \end{bmatrix} \vec{v}_{f,dq} \quad (11c)$$

$$C_{dc} \frac{dv_{dc}}{dt} = i_{dc} - \frac{3}{2} \left(\frac{m_d i_{cd}}{2} + \frac{m_q i_{cq}}{2} \right) \quad (11d)$$

C. Inclusion of Current Controller

Equations (6) and (11) define the converter dynamics in a time-periodic model and a time-invariant model, respectively. However, the models are not complete since the controller dynamics also need to be represented. The controller block diagram is given in Fig. 2.

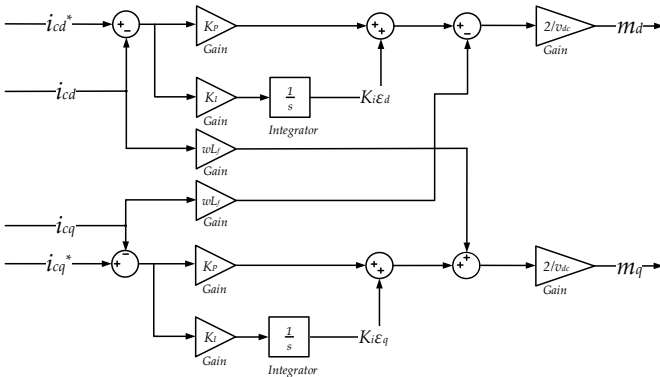


Fig. 2. Current controller block diagram

The states associated with the PI current controllers in the DQ frame are guided by the following error signals:

$$\frac{d\epsilon_d}{dt} = i_{cd}^* - i_{cd} \quad (12a)$$

$$\frac{d\epsilon_q}{dt} = i_{cq}^* - i_{cq} \quad (12b)$$

The current controllers create the modulation indices m_d and m_q as outputs, which are defined as:

$$m_d = \frac{K_P(i_{cd}^* - i_{cd}) + K_I\epsilon_d - \omega L_f i_{cq}}{\frac{v_{dc}}{2}} \quad (13a)$$

$$m_q = \frac{K_P(i_{cq}^* - i_{cq}) + K_I\epsilon_q + \omega L_f i_{cd}}{\frac{v_{dc}}{2}} \quad (13b)$$

The inclusion of the current controller in the time-invariant converter model is straightforward. However, for the time-periodic model in the ABC frame, one further step is needed for this control to convert the modulation indices in the DQ frame to their equivalents in the ABC frame, which is implemented as:

$$\vec{m}_{abc} = \begin{bmatrix} m_a \\ m_b \\ m_c \end{bmatrix} = \begin{bmatrix} \cos(\omega t) & \sin(\omega t) \\ \cos(\omega t - 2\pi/3) & \sin(\omega t - 2\pi/3) \\ \cos(\omega t - 4\pi/3) & \sin(\omega t - 4\pi/3) \end{bmatrix} \begin{bmatrix} m_d \\ m_q \end{bmatrix} \quad (14)$$

Equation 14 completes the time-periodic VSC model. With the current controller included, the time-invariant state-space VSC model in the DQ frame has 9 states, whereas the time-periodic state-space VSC model in the ABC frame has 12 states, with the state vectors defined as:

$$\vec{x}_{LTI} = [i_{gd} \ i_{gq} \ i_{cd} \ i_{cq} \ v_{fd} \ v_{fq} \ v_{dc} \ \epsilon_d \ \epsilon_q] \\ \vec{x}_{LTP} = [i_{ga} \ i_{gb} \ i_{gc} \ i_{ca} \ i_{cb} \ i_{cc} \ v_{fa} \ v_{fb} \ v_{fc} \ v_{dc} \ \epsilon_d \ \epsilon_q] \quad (15)$$

The details of the modeled converter are given in Table I.

TABLE I
CONVERTER DESIGN DATA.

Parameter	Description	Value
R_G	Grid-side resistance	0.012 Ω
L_G	Grid-side inductance	42.9 mH
R_F	Filter resistance	0.3429 Ω
L_F	Filter inductance	62.9 mH
C_F	Filter capacitance	2.3463 μF
C_{dc}	DC-side capacitance	62.7 μF
v_{dc}	Rated DC voltage	620.54 kV
$v_{g,LL}^{RMS}$	RMS value of the line voltage at the grid	380 kV
K_P	Current controller proportional gain	87.7171 V/A
K_I	Current controller integral gain	62900 V/As

IV. STABILITY ANALYSIS

A. Linearization at a Steady-State Operating Point

The models developed in the previous section become nonlinear with the inclusion of the controllers, since the modulation indices, which are functions of system states, are multiplied with the state variables. To conduct stability analysis based on the eigenvalues of the system matrix, the converter system including the controllers has to be linearized. The linearized system matrix is obtained by calculating the Jacobian of the system matrix and evaluating it at a steady-state operating point, and then its eigenvalues are calculated. When the Jacobian is evaluated at an operating point in which the AC grid voltage v_g and the DC-side voltage v_{dc} are at their nominal values and the d and q axis components of the converter current, i_{cd} and i_{cq} , are both controlled to -500 A, the corresponding eigenvalues of the LTI system are presented in Fig. 3.

For an LTI system to be stable in the small-signal sense, all its eigenvalues need to have negative real parts. This is exactly the case

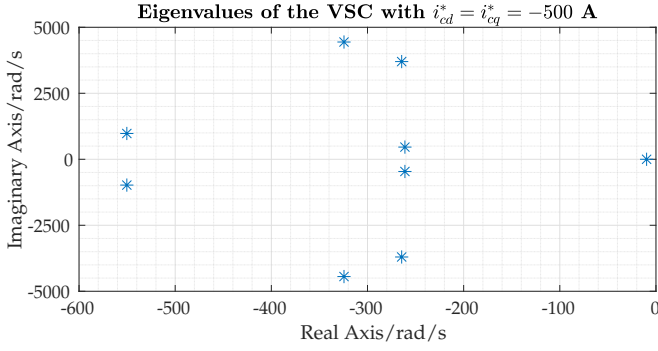


Fig. 3. Eigenvalues of the LTI model

in Fig. 3, which enables us to conclude that the two-level VSC with the specs given in Table I is stable in the small-signal sense at the operating point described above. In such a case, since both the LTI model and the LTP model are based on the same physical converter, one would expect to arrive at an LTP model that is also stable in the small-signal sense with the same converter and operating point properties. To validate this claim, the time-periodic model developed in Section III is linearized and its Poincaré multipliers are calculated at the same operating point by using the methodology introduced in Section II. The result is given in Fig. 4, together with the unit circle representing the stability limit.

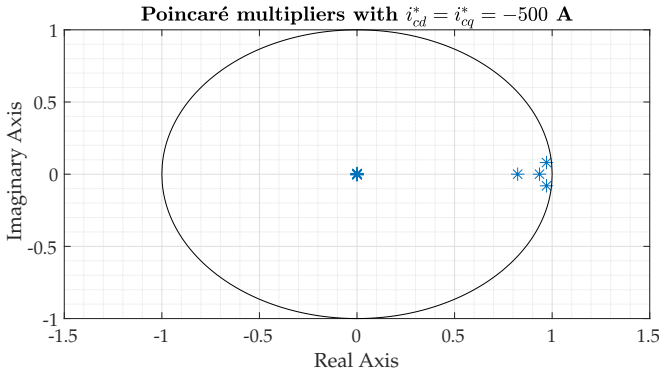


Fig. 4. Poincaré multipliers of the LTP model

The stability condition for the system in terms of its Poincaré multipliers is to have all of them lying inside the unit circle. We see that this is the case in Fig. 4, even though two of them are close to the stability limit. Hence, the LTP model of the VSC is also stable in the small-signal sense.

B. Variation of Controller Gains

Next, we analyze the impact of controller gains on the stability of the converter. We simulate a parametric sweep of the controller gains and observe the eigenvalue trajectories to independently define their effect. Specifically, the current controller gains K_P and K_I have been varied from 0 to twice their original values in both models. For the LTI model, results of these sweeps are given in Fig. 5 and Fig. 6. The eigenvalues with the original controller gains are depicted in turquoise.

It is observed that for different values of the proportional gain K_P , 8 eigenvalues show major changes, and they get closer to the stability limit for low K_P values. For the integral gain K_I , only four eigenvalues show major changes, and two of them come closer to the origin for low values of K_I .

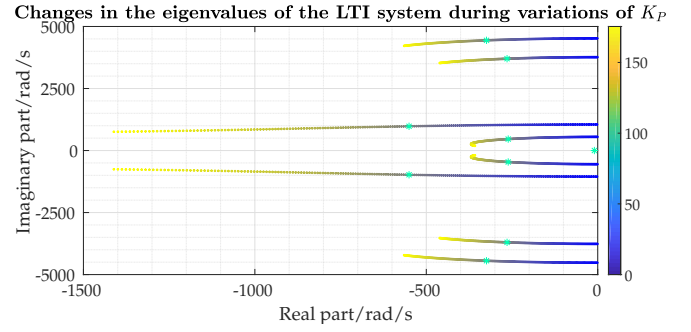


Fig. 5. Trajectories of the LTI system eigenvalues during variations of K_P

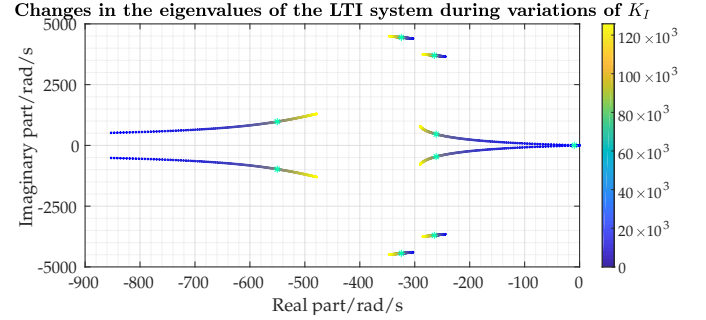


Fig. 6. Trajectories of the LTI system eigenvalues during variations of K_I

For the LTP model, the trajectories of the Poincaré multipliers during the same sweep are given in Fig. 7 and Fig. 8. The multipliers with the original gains are plotted in turquoise.

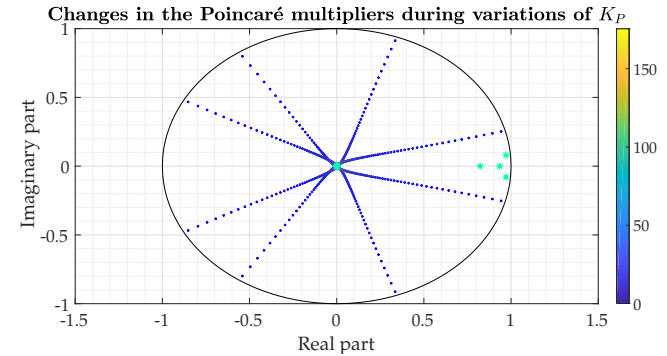


Fig. 7. Trajectories of the Poincaré multipliers of the LTP system during variations of K_P

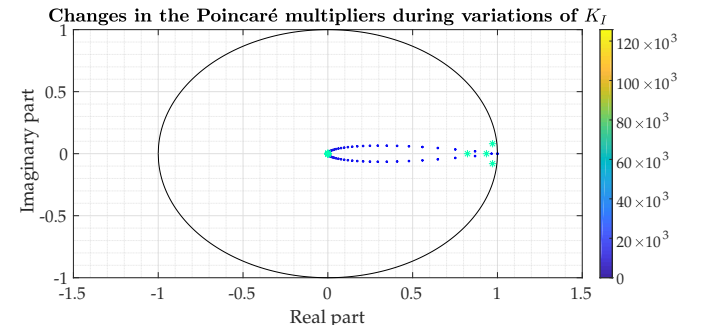


Fig. 8. Trajectories of the Poincaré multipliers of the LTP system during variations of K_I

Similar to the LTI model, for low values of K_P 8 out of 12 Poincaré multipliers grow in magnitude, thereby getting closer to the unit circle indicating the stability limit. For the variations in K_I , two multipliers show major changes, moving towards the point (1,0).

As a result of the parameter variations presented above, we conclude that both models can effectively represent the small-signal stability behavior of a two-level VSC. Variations in the converter parameters result in similar changes for the eigenvalues of the LTI model and the Poincaré multipliers of the LTP model. When both approaches are compared, it can be said that the LTI model is more preferable since it offers the possibility to discover the inherent oscillatory modes of the system and associate them with system states through modal analysis, a feature which is not commonly applied to LTP systems [8]. In modal analysis, the participation factors are calculated from the left eigenvectors w and the right eigenvectors v . Different definitions of the participation factors exist, yet in this paper, the approach of Abed *et al.* is followed, which results in real values for participation factors [9]. For an arbitrary eigenvalue λ_i , its participation factor associated with state j is calculated as:

$$P_{ij} = \begin{cases} v_{ij}w_{ij} & \text{if } \lambda_i \in \mathbb{R} \\ 2\text{Re}(v_{ij})\text{Re}(w_{ij}) & \text{if } \lambda_i \in \mathbb{C} \end{cases} \quad (16)$$

The application of modal analysis to the system with the original gains helps us associate the converter eigenvalues with the system states. The results for the 5 states that have the maximum impact on the eigenvalues are given in Table II.

TABLE II
PARTICIPATION FACTORS OF THE EIGENVALUES OF THE LTI MODEL.

Eigenvalue/rad/s	State 1		State 2		State 3		State 4		State 5	
	Name	PF/%	Name	PF/%	Name	PF/%	Name	PF/%	Name	PF/%
-9.72	v_{dc}	100								
$-324.44 \pm 4442.29j$	v_{fq}	49.57	i_{gd}	28.34	i_{cd}	22.65	ϵ_q	1.18		
$-264.45 \pm 3700.98j$	v_{fq}	50.75	i_{gd}	30.88	i_{cd}	18.35	ϵ_q	1.37		
$-550.30 \pm 977.30j$	i_{cd}	27.11	i_{gd}	18.16	i_{cq}	17.68	ϵ_q	16.78	i_{gq}	11.55
$-261.09 \pm 461.97j$	ϵ_q	41.61	ϵ_d	29.88	i_{cd}	9.96	i_{gd}	7.11	i_{cq}	6.66

From the participation factors depicted in Table II, we see that the eigenvalue at -9.72 is solely associated with the DC voltage, therefore if a DC voltage controller is added to the system, its small-signal stability can be significantly improved.

V. THE IMPACT OF THE CONTROL ARCHITECTURE

In this paper, the converter current of a two-level VSC is controlled by means of PI controllers in the DQ frame. Since the DQ frame is rotating with the same frequency as the converter current of the VSC, the variables appear as constants in the DQ frame. This will also be the case if proportional-resonant (PR) controllers at the fundamental frequency are used to control the sinusoidal currents: the controller signals, which oscillate with the fundamental frequency, can be transformed to the DQ frame, even though the controllers that are being used are not based on that frame. However, such a transform is only applicable in case of a three-phase VSC. Moreover, in case the controller generates signals at frequencies other than the fundamental frequency, such as the controllers used for active filtering or negative-sequence current injection applications, the controller variables in the DQ frame are not constants during steady state, resulting in a time-varying system. Therefore, a linearized converter model utilizing variables on a DQ frame rotating with the fundamental grid frequency might not always result in a time-invariant system.

Conversely, if such time-periodicity is allowed in the system by carrying out the stability analysis using the linear time-periodic

framework, no problems will be faced since as long as the period of the system matrix is known, the Poincaré multipliers can be calculated to assess the small-signal stability of the system. Hence, the usage of the LTP framework brings up the possibility of studying the small-signal stability of single-phase converters and a much broader family of converter controllers.

VI. CONCLUSIONS

This paper introduced a comparison of different small-signal modeling and stability analysis methods for power-electronic converters, namely the LTI framework and the LTP framework. Following introductions of the theoretical background of both methodologies, time-invariant and time-periodic models were developed for a three-phase two-level VSC. After linearization, the eigenvalues of the LTI model and the Poincaré multipliers of the LTP system—the eigenvalues of its state-transition matrix—are illustrated for a steady-state operating point in which the voltages are at their nominal values and the d and q axis currents are both controlled to -500 A. Finally, both models are used to assess the effect of the controller gains on the small-signal stability of the system by varying the controller gains. It was observed that in both models, the eigenvalues and the multipliers approached stability limits for extreme values of the controller gains, the limits being the imaginary axis for LTI systems and the unit circle for LTP systems. A discussion on the impact of the chosen control architecture revealed that even though the LTI framework seems to provide more insight regarding the stability of the converter through modal analysis methods, the LTP framework might be inevitable to study the small-signal stability of certain controller architectures. Future research will be focusing on the inclusion of additional controllers to the system, the extension of the LTP framework to the stability analysis of more complicated converter topologies and tools that can provide further insight on stability when the LTP framework is being used.

REFERENCES

- [1] M. Amin and M. Molinas, "Small-signal stability assessment of power electronics based power systems: A discussion of impedance- and eigenvalue-based methods," *IEEE Transactions on Industry Applications*, vol. 53, pp. 5014–5030, Sept 2017.
- [2] P. Kundur, N. Balu, and M. Lauby, *Power system stability and control*. EPRI Power System Engineering Series, McGraw-Hill, 1994.
- [3] M. Montagnier, R.J. Spiteri, and J. Angeler, "The control of linear time-periodic systems with Floquet-Lyapunov theory," *Int. J. Control*, vol. 77, pp. 472–490, Jan 2004.
- [4] A. Yazdani and R. Iravani, *Voltage-Sourced Converters in Power Systems: Modeling, Control, and Applications*. Wiley, 2010.
- [5] N. R. Chaudhuri, R. Oliveira, and A. Yazdani, "Stability analysis of vector-controlled modular multilevel converters in linear time-periodic framework," *IEEE Transactions on Power Electronics*, vol. 31, pp. 5255–5269, July 2016.
- [6] S. K. Mazumder, A. H. Nayfeh, and D. Boroyevich, "A novel approach to predict the instabilities and analyze the dynamics of a single phase bidirectional boost converter," in *Proceedings of the 2002 IEEE 33rd Annual IEEE Power Electronics Specialists Conference. (Cat. No.02CH37289)*, vol. 4, pp. 1711–1716, 2002.
- [7] O. Dranga, B. Buti, and I. Nagy, "Stability analysis of a feedback-controlled resonant DC-DC converter," *IEEE Transactions on Industrial Electronics*, vol. 50, pp. 141–152, Feb 2003.
- [8] I. J. Perez-arriaga, G. C. Verghese, and F. C. Schwegge, "Selective modal analysis with applications to electric power systems, PART I: heuristic introduction," *IEEE Transactions on Power Apparatus and Systems*, vol. PAS-101, pp. 3117–3125, Sept 1982.
- [9] E. H. Abed, M. A. Hassouneh, and W. A. Hashlamoun, "Modal participation factors revisited: One definition replaced by two," in *Proceedings of the 2009 American Control Conference*, pp. 1140–1145, June 2009.